ELSEVIER

Nuclear Instruments and Methods in Physics Research A 471 (2001) 209–214

NUCLEAR INSTRUMENTS & METHODS IN PHYSICS RESEARCH Section A

www.elsevier.com/locate/nima

Trends in PET imaging ☆

William W. Moses*

Lawrence Berkeley National Laboratory, University of California, Mailstop 55-121, 1 Cyclotron Road, Berkeley, CA 94720, USA

Abstract

Positron Emission Tomography (PET) imaging is a well established method for obtaining information on the status of certain organs within the human body or in animals. This paper presents an overview of recent trends in PET instrumentation. Significant effort is being expended to develop new PET detector modules, especially those capable of measuring the depth of interaction. This is aided by recent advances in scintillator and pixellated photodetector technology. The other significant area of effort is in the development of special purpose PET cameras (such as for imaging breast cancer or small animals) or cameras that have the ability to image in more than one modality (such as PET/SPECT or PET/X-ray CT). © 2001 Elsevier Science B.V. All rights reserved.

Keywords: PET; PET instrumentation

1. Introduction

Positron Emission Tomography (PET) is a nuclear medical imaging technique whereby a biologically active compound (i.e. a drug) labeled with a positron emitting isotope (usually ^{18}F, ^{11}C, ^{13}N, or ^{15}O) is introduced into the body (in trace quantities) either by injection or inhalation. This compound then accumulates in the patient and the pattern of its subsequent radioactive emissions is used to estimate the distribution of the radioisotope and hence of the tracer compound [1–7].

Since the image that is produced is of the distribution of a drug within the body, PET is capable of targeting where certain metabolic processes occur and measuring the rate at which these processes take place. Thus, it is able to determine whether the biochemical function of an organ is impaired, while many other forms of medical imaging (such as X-ray, ultrasound, or magnetic resonance techniques) are usually confined to determining the physical structure of the organ. It is therefore most frequently used in organs and diseases where biological function is of primary importance and information on physical structure is either irrelevant or ambiguous. Examples are neurological diseases (such as Alzheimer's disease) where physical affects are only observable on a microscopic level, heart disease (where the relative vigor of the tissue is of primary importance), or oncology (cancer), where the metabolic

☆This work was supported in part by the US Department of Energy under Contract No. DE-AC03-76SF00098, and in part by Public Health Service Grant Nos. R01-CA67911 and P01-HL25840 from the National Institutes of Health.

*Tel.: +1-510-486-4432; fax: +1-510-486-4768.

E-mail address: wwmoses@lbl.gov (W.W. Moses).

PII: S0168-9002(01)00969-X

rate gives valuable information on whether the tissue is cancerous and how it responds to treatment.

A typical PET camera consists of a planar ring of small photon detectors, with each photon detector placed in time coincidence with *each* of the individual photon detectors on the other side of the ring (Fig. 1). When a pair of photon detectors simultaneously detect 511 keV photons, a positron is known to have annihilated somewhere on the line connecting the two detectors. The set of all lines connecting detectors (known as chords) makes the requisite set of projections to perform computed tomography for a single plane. Multiple detector rings are stacked on top of each other to obtain images from multiple slices, and thus a three-dimensional image of the patient. Planes of tungsten septa placed between detector planes are often used to shield the detectors from Compton scattered photons emanating from other parts of the body, and images taken in this geometry are often known as "2-D PET" images. The coincidences between nearly adjacent "cross-plane" rings are usually added to the closest "direct plane" to increase detection efficiency. If the septa are removed, the efficiency is greatly increased (as coincidences from widely separated planes can be accepted), but the backgrounds also increase significantly. However, the signal to noise ratio improves in some situations, and this mode of operation is known as "3-D PET".

2. PET detector module trends

The most commonly used PET detector module is known as a block detector, a schematic of which is shown in Fig. 2 [8]. A block of BGO scintillator crystal is partially sawn through to make a group of quasi-independent crystals that are optically coupled to four photomultiplier tubes. When a gamma ray interacts in the crystal, the resulting scintillation photons are emitted isotropically but the saw cuts limit (but do not entirely prevent) their lateral dispersion as they travel toward the photomultiplier tubes. The position (i.e. crystal element) of the gamma ray interaction is then determined by the analog ratio of the photomultiplier tube output signals, and the gamma ray energy is determined and a timing pulse generated by the sum of these four signals. A typical PET detector module has 80% detection efficiency, 20% FWHM energy resolution, 2 ns FWHM timing resolution, 4 μs dead time, and 5 mm FWHM position resolution for 511 keV gammas [9].

The detector module performance is limited by the BGO scintillator crystal. A scintillator with a faster decay time would improve the timing resolution and decrease dead time, while one with a higher light output would improve the energy resolution and spatial resolution (by allowing more crystals per block to be unambiguously

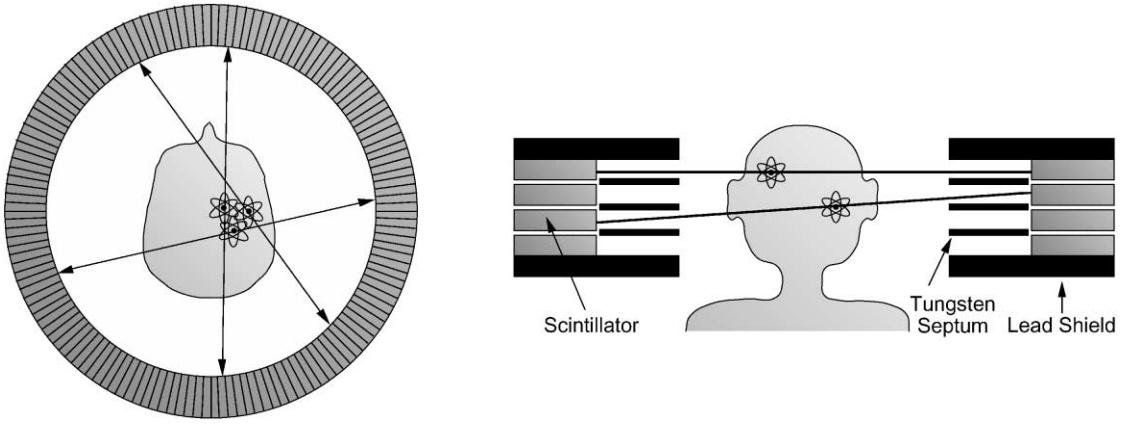

Fig. 1. PET camera. The diagram on the left shows a single plane of a PET camera, consisting of a ring of gamma detectors placed around the object to be imaged. When the crystals in opposing hemispheres simultaneously detect 511 keV gammas, a positron is assumed to have annihilated on the line connecting them. Multiple planes are stacked up, as shown on the right to form a volumetric image. Tungsten septa reduce out-of-plane contributions.

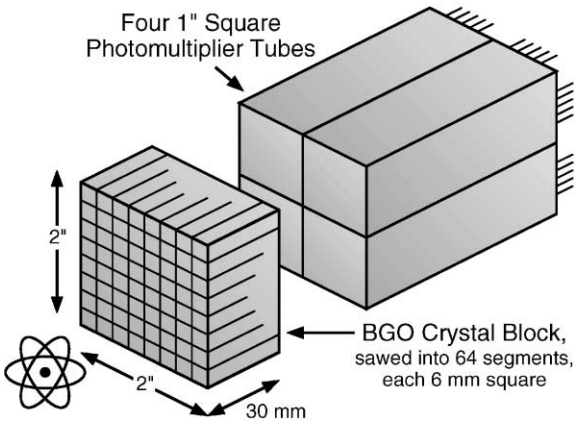

Fig. 2. Conventional PET detector module. Scintillation light from gamma ray interactions is detected by multiple photomultiplier tubes. The interaction position is determined by the ratio of the analog signals, and the energy by the analog sum of the signals.

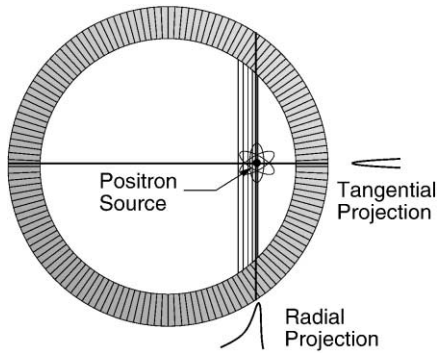

Fig. 3. Cause of radial elongation: 511 keV photons that are incident at an oblique angle can penetrate into the detector ring before interacting and being detected. This causes a blurring that worsens as the source is moved away from the center of the ring.

decoded). However, a short attenuation length is critical in order to maintain a high spatial resolution (the details are described in the following paragraph), and for this reason BGO dominates. However, some recently developed scintillators are being incorporated into experimental PET systems. Cerium activated lutetium orthosilicate (Lu_2SiO_5:Ce or LSO) exhibits four times higher light output and eight times faster decay time than BGO, while maintaining a similar attenuation length [10]. Although it has self-induced background events from naturally occurring ^{176}Lu, its use for PET is compelling and there is hope that the cost can be reduced enough to make it viable. LSO has been used for a large number of prototype PET detector module designs and a high resolution research PET camera has been made with LSO [11]. Gadolinium orthosilicate (Gd_2SiO_5:Ce or GSO) has 50% higher light output than BGO and five times faster decay time, but its attenuation length is 40% longer [12]. This, in addition to a cleavage plane that makes fabrication difficult makes GSO a less compelling alternative than LSO, but a brain PET camera using GSO is under construction [13].

In order to increase the efficiency and reduce the number of detector modules (and hence cost), PET camera designers would like to reduce the diameter of the detector ring. Unfortunately, they are prevented from doing this by a resolution degradation artifact caused by the penetration of the 511 keV photons into the crystal ring. The origin of this artifact, variously known as radial elongation, parallax error, or radial astigmatism, is shown in Fig. 3. Photons that impinge on the detector ring at an oblique angle can penetrate into adjacent crystals before they interact and are detected, which causes mispositioning errors (i.e. events are assigned to chords that do not pass through the source). This spatial resolution degradation increases for objects placed further away from the center of the tomograph ring. This artifact can be reduced significantly or eliminated if the detector module is capable of measuring not only the identity of the crystal of interaction but the depth of the interaction within that crystal. With such information, the event can be assigned to the chord that connects the interaction points (rather than the interaction crystals), and as that chord will pass through the source, no mispositioning errors are generated.

Developing a detector module capable of accurately measuring this interaction depth is an active field of research. Fig. 4 schematically shows three general approaches that have been taken to measure interaction depth. The first, shown in Fig. 4a, is a phoswich approach, in which the scintillator block of a conventional PET detector is

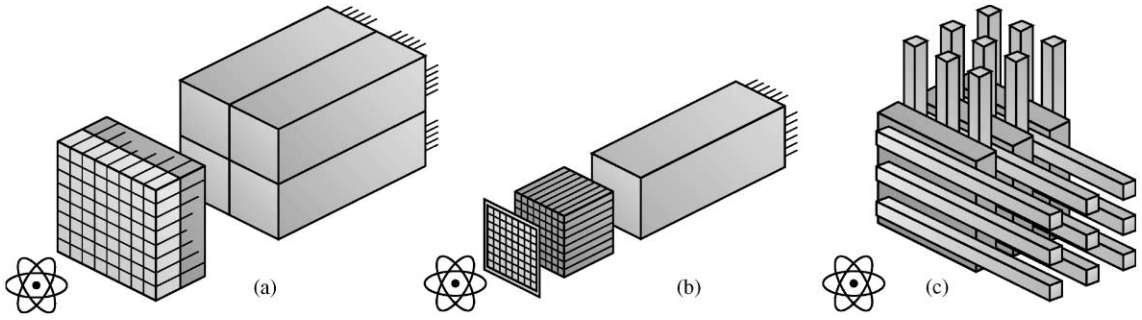

Fig. 4. Depth of interaction measurement concepts. In (a), the scintillator in a conventional PET detector module is stratified in depth with two different scintillator materials—the depth is distinguished by decay time. In (b), scintillation light is shared between two photodetectors—the ratio determines the depth. The detector in (c) is comprised of a stack of imaging planes—the depth is determined by the layer at which the interaction is observed.

effectively replaced with two or more layers of different scintillator materials, so each scintillator "pixel" now contains stratified layers of scintillator material [14]. As the different materials possess different scintillation decay times, the readout electronics is modified to perform a crude measurement of the decay time, and so the type of the scintillator that the interaction occurred in (and therefore the interaction depth) is identified. A high resolution research PET camera that utilizes a 15 mm deep phoswich detector made of 7.5 mm deep LSO and GSO crystals has recently been built [15].

The second general technique for measuring the depth of interaction, shown in Fig. 4b, is to utilize light sharing. With this approach, each scintillator element is attached to two photodetectors, usually on opposing ends of the crystal. The amount of light observed by each photodetector depends on the interaction position, so the ratio of the two photodetector signals is used to estimate the interaction depth. Recent advances in pixellated photodetectors have contributed greatly to this design approach. Many combinations of photodetectors have been used, including single anode photomultiplier tubes, PIN photodiode arrays, avalanche photodiode arrays, and multianode photomultiplier tubes [16–19]. At present, no cameras have been built utilizing any of these schemes, although several are under construction.

The third approach for measuring the interaction depth, shown in Fig. 4c, is to stack multiple layers of two-dimensional detector planes. The plane that the interaction is observed in identifies the depth while a 2-D detector provides the other two coordinates. One proposed 2-D detector consists of orthogonal arrays of wavelength-shifting fibers coupled to thin plates of LSO scintillator crystal [20,21]. The fiber absorbs this primary scintillation light and re-emits lower energy photons, some of which are transported down the length of the fiber and are observed by a position-sensitive photodetector. Another 2-D detector that has been incorporated into a PET camera consists of many thin sheets of lead interspersed with wire chambers [22,23]: 511 keV interactions in the lead result in some recoil electrons entering the active area of the wire chamber, where they are detected. Such detectors have an excellent spatial resolution, but sacrifice both detection efficiency and energy resolution.

3. Trends in PET camera design

The biggest current trends in PET camera design are specific purpose cameras and cameras that are capable of imaging with two modalities. Conventional whole-body PET cameras can image any part of the body. Their development is mature enough such that the main gains to be made are in the cost/performance tradeoff, where only relatively small gains are possible. However, cameras can be optimized for imaging a single organ, which could result in large performance gains at the expense of a limited body coverage. A prime

example of this is PET cameras optimized for imaging breast cancer, for which there are a number of designs [24–27]. Another field that is growing rapidly is PET cameras for imaging small animals, especially mice and rats. PET's ability to measure biochemical function, rather than structure, can provide crucial insight into the functioning of new and existing pharmaceuticals, the nature of diseases, or the function of specific genes. These experiments are usually performed in small animals, requiring resolutions much higher than those achieved in human PET scanners. By using small scintillator crystals and multianode photomultiplier tubes, spatial resolutions below 2 mm FWHM have been achieved [28–32].

It is often desirable to perform different types of imaging procedures on a single patient. For example, X-ray CT provides excellent anatomical details while PET provides biochemical information—obtaining both images of the same patient is likely to lead to a more accurate diagnosis than either single image would. Thus, devices have recently been built in which an X-ray CT imager and a PET imager have been placed around a single patient bed [33]. While images from both modalities cannot be obtained simultaneously, the ability to perform both studies without repositioning the patient is extremely helpful, especially when imaging the abdomen.

Finally, there has been a strong trend in recent years to equip SPECT cameras (which are optimized to detect 140 keV gamma rays) with coincidence electronics and give them the ability to obtain PET images. The benefits of this are largely economic—SPECT cameras are far more common than dedicated PET cameras and so any hospital with a SPECT camera can, for a relatively small cost, also have the ability to acquire PET images. Some compromises in performance (as compared to dedicated PET cameras) are necessary, but clinically valuable images are often obtained.

4. Conclusion

PET imaging has benefited from recent developments in scintillator materials and pixellated photodetectors, which have enabled a number of detector module designs that are capable of measuring the depth of interaction. By measuring the depth of interaction, PET camera makers can maintain a high spatial resolution with smaller detector ring diameters, simultaneously reducing cost and increasing performance. Recent years have also seen the emergence of special purpose PET cameras, notably for imaging breast cancer or small animals, as well as cameras that also have the ability to obtain SPECT or X-ray CT images.

Acknowledgements

I would like to thank Dr. Stephen Derenzo, Dr. Thomas Budinger, and Dr. Ronald Huesman for many interesting conversations, and would also like to thank Dr. Mats Danielsson for the opportunity to consider the current trends in PET imaging. This work was supported in part by the Director, Office of Science, Office of Biological and Environmental Research, Medical Science Division of the US Department of Energy under Contract No. DE-AC03-76SF00098, and in part by the National Institutes of Health, National Cancer Institute under grant No. R01-CA67911, and National Institutes of Health, National Heart, Lung, and Blood Institute under grant No. P01-HL25840.

References

[1] Special Issue on Clinical PET, J. Nucl. Med. 32 (1991) 561.
[2] M.P. Sandler, R.E. Coleman, F.J.T. Wackers, et al., Diagnostic Nuclear Medicine, Williams & Wilkins, Baltimore, MD, 1996.
[3] W.R. Hendee, R. Ritenour, Medical Imaging Physics, Mosby Year Book, St. Louis, MO, 1992.
[4] E. Krestel, Imaging Systems for Medical Diagnosis, Siemens Aktiengesellschaft, Berlin, 1990.
[5] A. Macovski, Medical Imaging Systems, Prentice-Hall, Englewood Cliffs, NJ, 1983.
[6] S. Webb, The Physics of Medical Imaging, Institute of Physics Publishing, Bristol, 1993.
[7] S.R. Cherry, M.E. Phelps, Positron emission tomography: Methods and instrumentation, in: M.P. Sandler, R.E. Coleman, F.J.T. Wackers, J.A. Patton, A. Gottschalk, P.B. Hoffer (Eds.), Diagnostic Nuclear Medicine, Williams & Wilkins, Baltimore, MD, 1996, pp. 139–159.

[8] S.R. Cherry, M.P. Tornai, C.S. Levin, et al., IEEE Trans. Nucl. Sci. NS-42 (1995) 1064.
[9] W.W. Moses, S.E. Derenzo, T.F. Budinger, Nucl. Instr. and Meth. A 353 (1994) 189.
[10] C.L. Melcher, J.S. Schweitzer, IEEE Trans. Nucl. Sci. NS-39 (1992) 502.
[11] M. Schmand, K. Wienhard, M.E. Casey, et al., Performance evaluation of a new LSO high resolution research tomograph-HRRT, in: J.A. Seibert (Ed.), Proceedings of the IEEE 1999 Nuclear Science Symposium and Medical Imaging Conference, Vol. 2, Seattle, WA, 1999, Paper M04-002, pp. 1067–1071.
[12] K. Takagi, T. Fukazawa, Appl. Phys. Lett. 42 (1983) 43.
[13] J.S. Karp, L.E. Adam, R. Freifelder, et al., A high-resolution GSO-based brain PET camera, in: J. A. Seibert (Ed.), Proceedings of the IEEE 1999 Nuclear Science Symposium and Medical Imaging Conference, Vol. 2, Seattle, WA, 1999, pp. 1077–1081.
[14] A. Saoudi, C.M. Pepin, F. Dion, et al., IEEE Trans. Nucl. Sci. NS-46 (1999) 462.
[15] M. Schmand, L. Eriksson, M. Casey, et al., IEEE Trans. Nucl. Sci. NS-45 (1998) 3000.
[16] J.S. Huber, W.W. Moses, M.S. Andreaco, et al., A LSO scintillator array for a PET detector module with depth of interaction measurement, IEEE Trans. Nucl. Sci. NS-48 (2001) in press.
[17] Y.P. Shao, S.R. Cherry, IEEE Trans. Nucl. Sci. NS-46 (1999618).
[18] J.G. Rogers, C. Moisan, E.M. Hoskinson, et al., IEEE Trans. Nucl. Sci. NS-43 (1996) 3240.
[19] R.S. Miyaoka, T.K. Lewellen, J.H. Yu, et al., IEEE Trans. Nucl. Sci. NS-45 (1998) 1069.
[20] W. Worstell, O. Johnson, H. Kudrolli, et al., IEEE Trans. Nucl. Sci. 45 (1998) 2993.
[21] M.B. Williams, R.M. Sealock, S. Majewski, et al., IEEE Trans. Nucl. Sci. 45 (1998) 195.
[22] A.P. Jeavons, R.A. Chandler, C.A.R. Dettmar, IEEE. Trans. Nucl. Sci. NS-46 (1999) 468.
[23] V. Chepel, V. Solovov, J. van der Marel, et al., IEEE Trans. Nucl. Sci. NS-46 (1999) 1038.
[24] K. Murthy, M. Aznar, A.M. Bergman, et al., Radiology 215 (2000) 280.
[25] N.K. Doshi, Y.P. Shao, R.W. Silverman, et al., Med. Phys. 27 (2000) 1535.
[26] R. Freifelder, J.S. Karp, Phys. Med. Biol. 42 (1997) 2463.
[27] W.W. Moses, T.F. Budinger, R.H. Huesman, et al., J. Nucl. Med. 36 (1995) 69.
[28] A.F. Chatziioannou, S.R. Cherry, Y.P. Shao, et al., J. Nucl. Med. 40 (1999) 1164.
[29] A. Del Guerra, C. Damiani, G. Di Domenico, et al., IEEE Trans. Nucl. Sci. NS-47 (2000) 1537.
[30] A.P. Jeavons, J. Nucl. Med. 41 (2000) 1442.
[31] S. Siegel, J.J. Vaquero, L. Aloj, et al., IEEE Trans. Nucl. Sci. NS-46 (1999) 571.
[32] D. Lapointe, N. Brasseur, J. Cadorette, et al., J. Nucl. Med. 40 (1999) 876.
[33] T. Beyer, D.W. Townsend, T. Brun, et al., J. Nucl. Med. 41 (2000) 1369.